Electronic Supplementary Information (ESI) for

Porphyrin Chemodosimeters: Synthesis, Electrochemical Redox Properties and Selective 'Naked-eye' Detection of Cyanide Ions

Mandeep K. Chahal and Muniappan Sankar*

Department of Chemistry, Indian Institute of Technology Roorkee, Roorkee-247667, India

Table of Contents

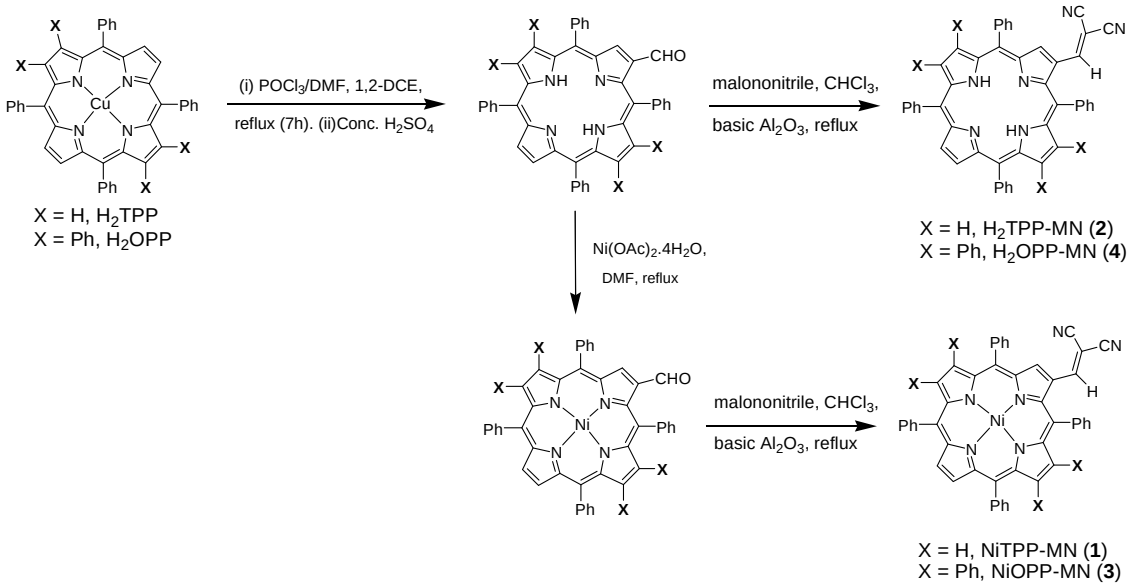

Scheme S1. Synthetic route to dicyanovinyl appended β-substituted porphyrins (**1-4**).

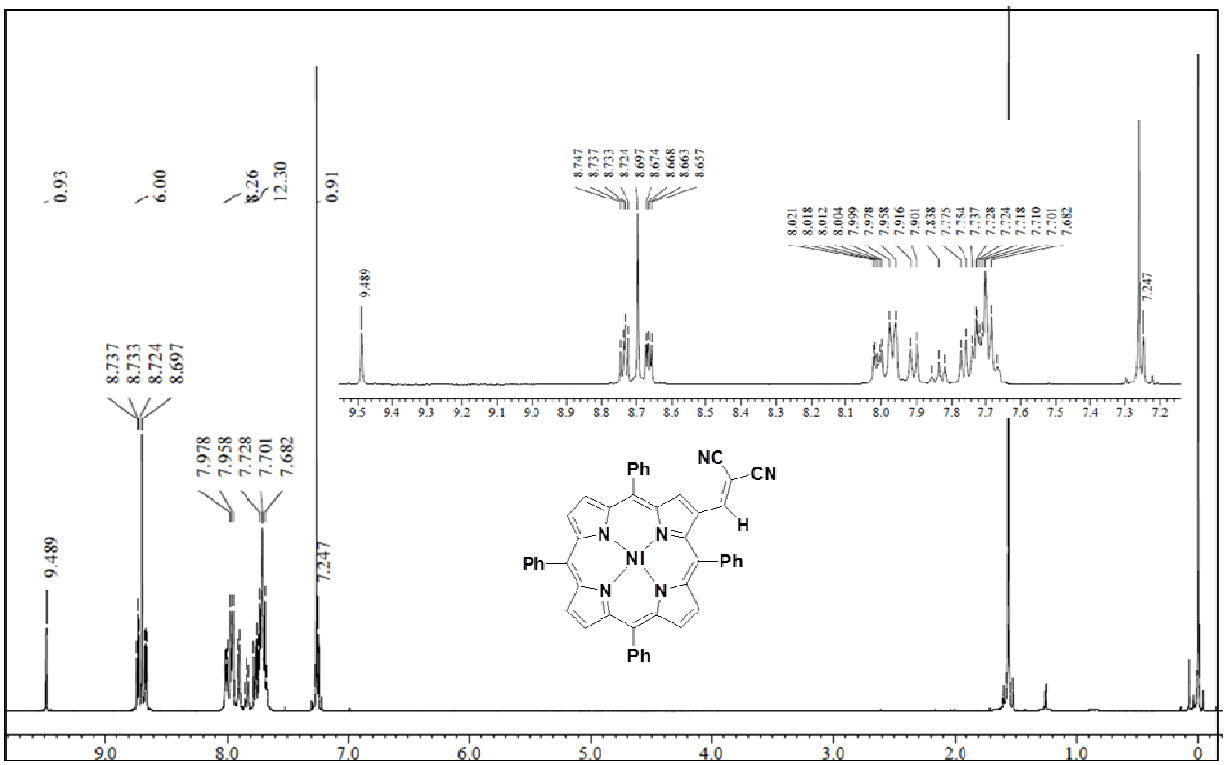

Figure S1. ^{1}H NMR spectrum of NiTPP-MN (**1**).

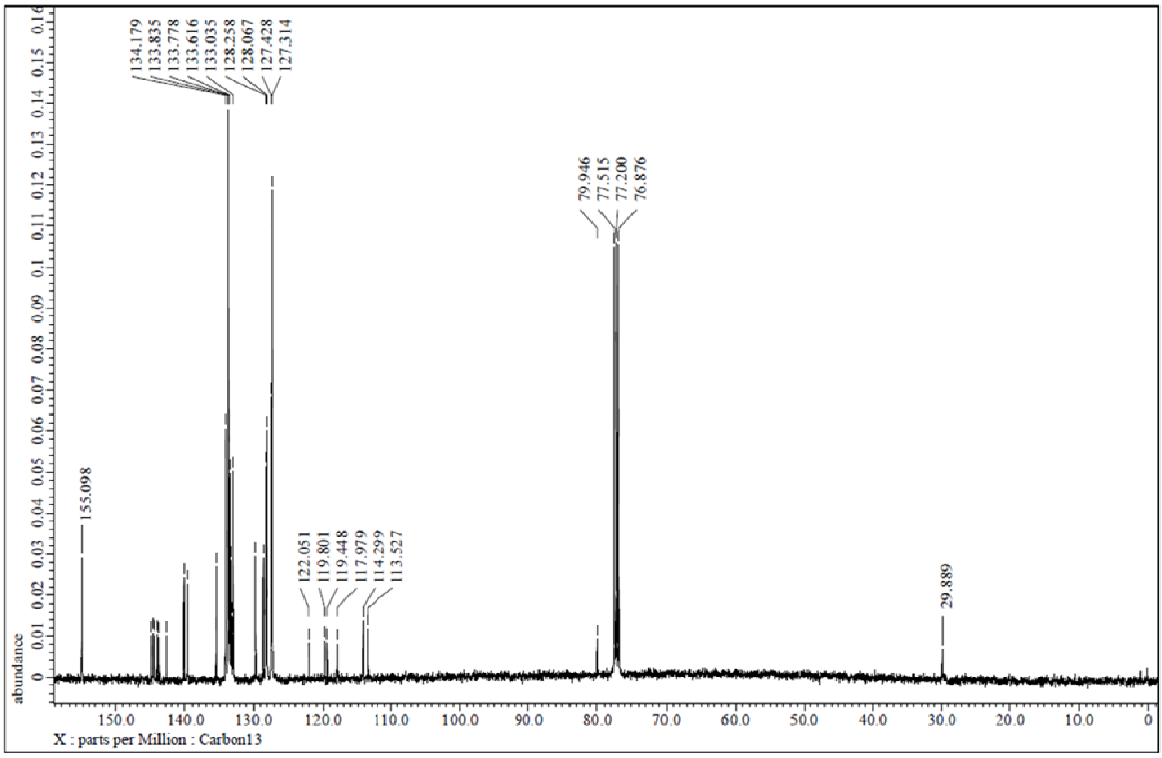

Figure S2. ^{13}C NMR spectrum of NiTPP-MN (**1**).

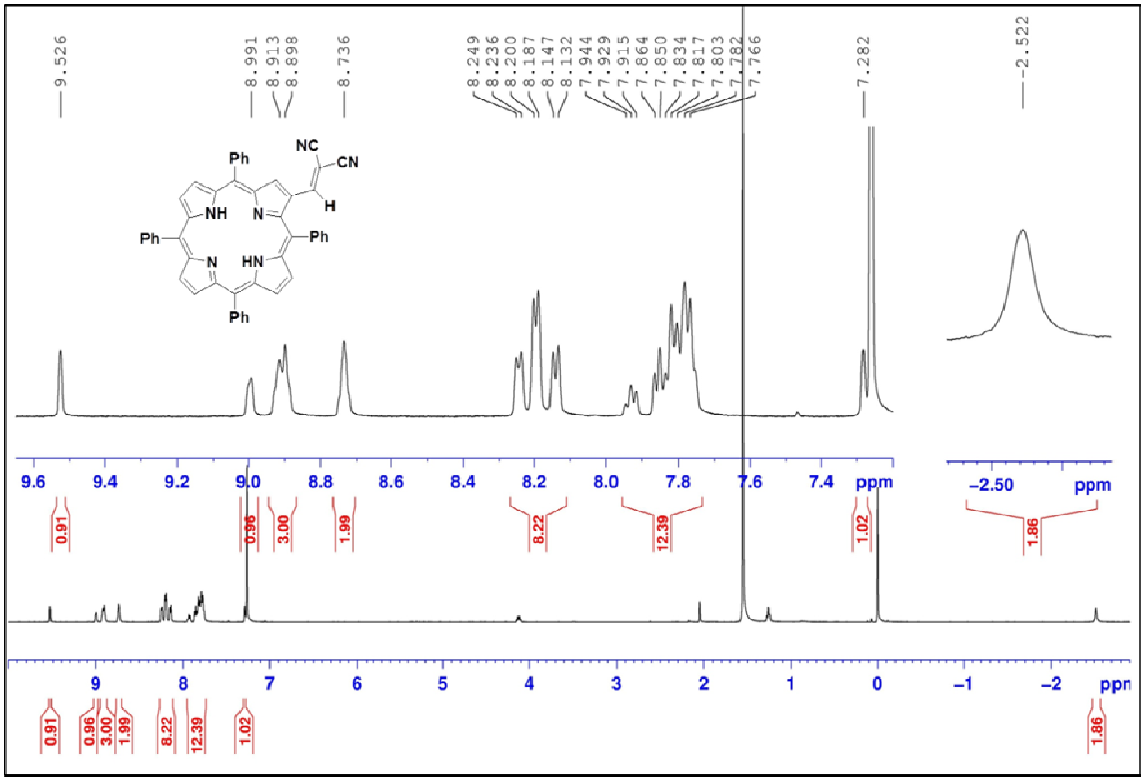

Figure S3. ^{1}H NMR spectrum of H_2TPP-MN (**2**).

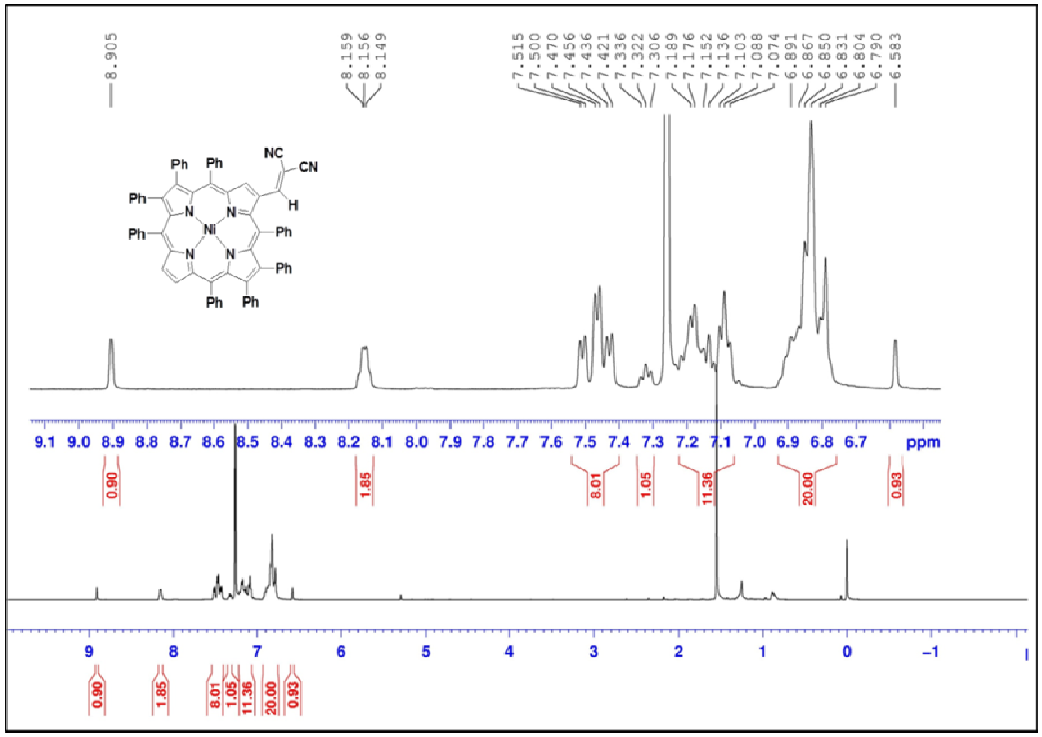

Figure S4. ^{1}H NMR spectrum of NiOPP-MN (**3**).

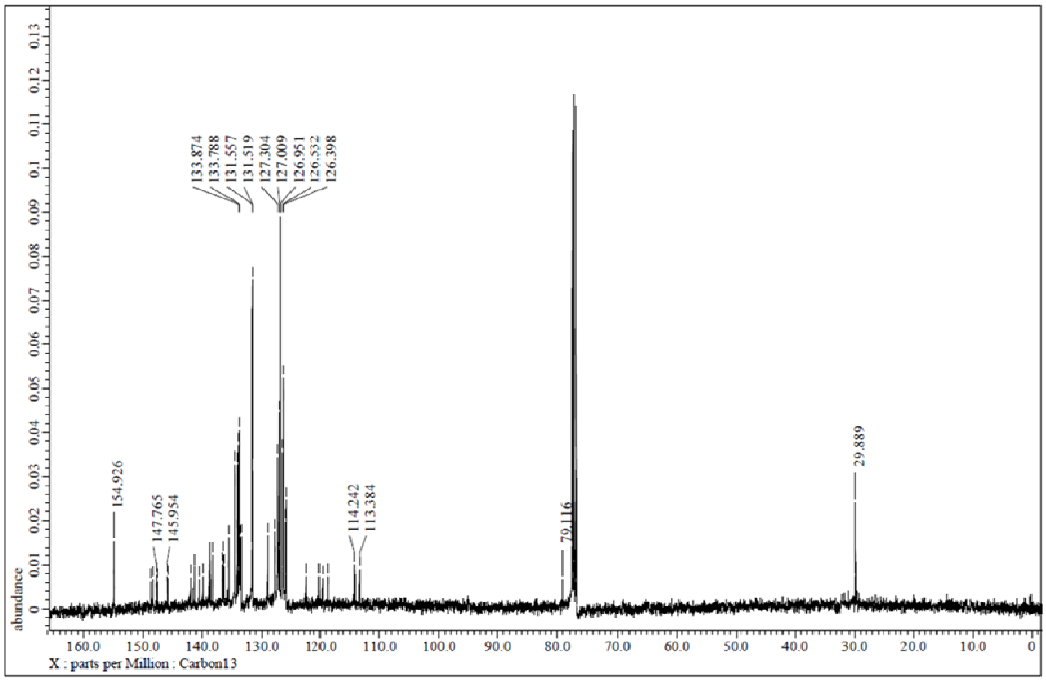

Figure S5. ^{13}C NMR spectrum of NiOPP-MN (**3**).

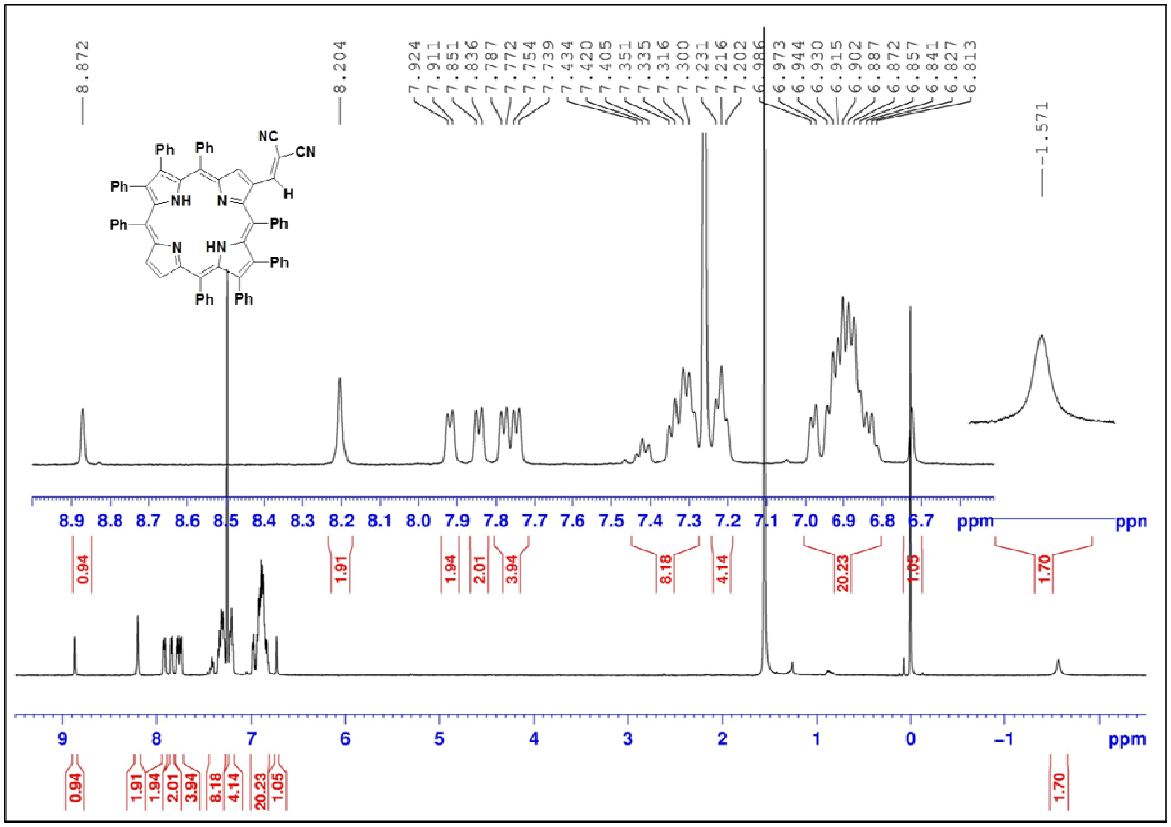

Figure S6. ^{1}H NMR spectrum of H_2OPP-MN (**4**).

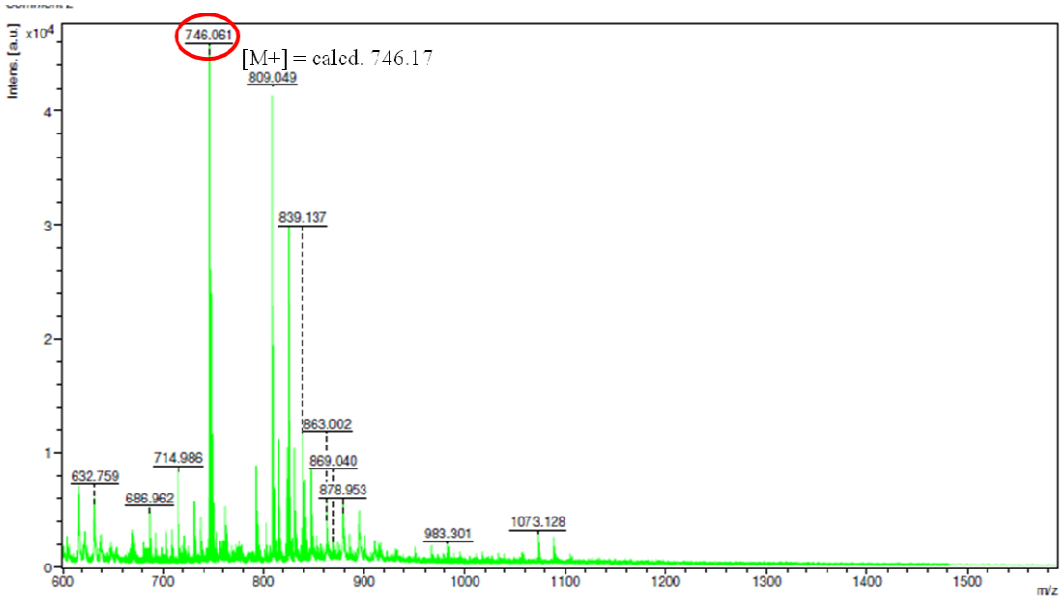

Figure S7. MALDI-TOF mass spectrum of NiTPP-MN (**1**).

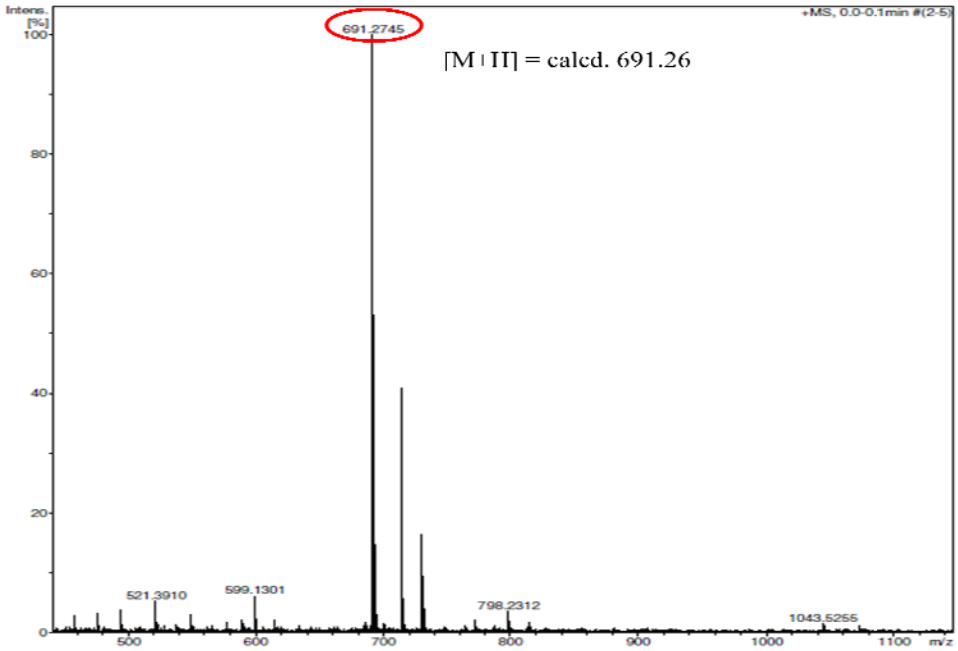

Figure S8. ESI mass spectrum of H_2TPP-MN (**2**).

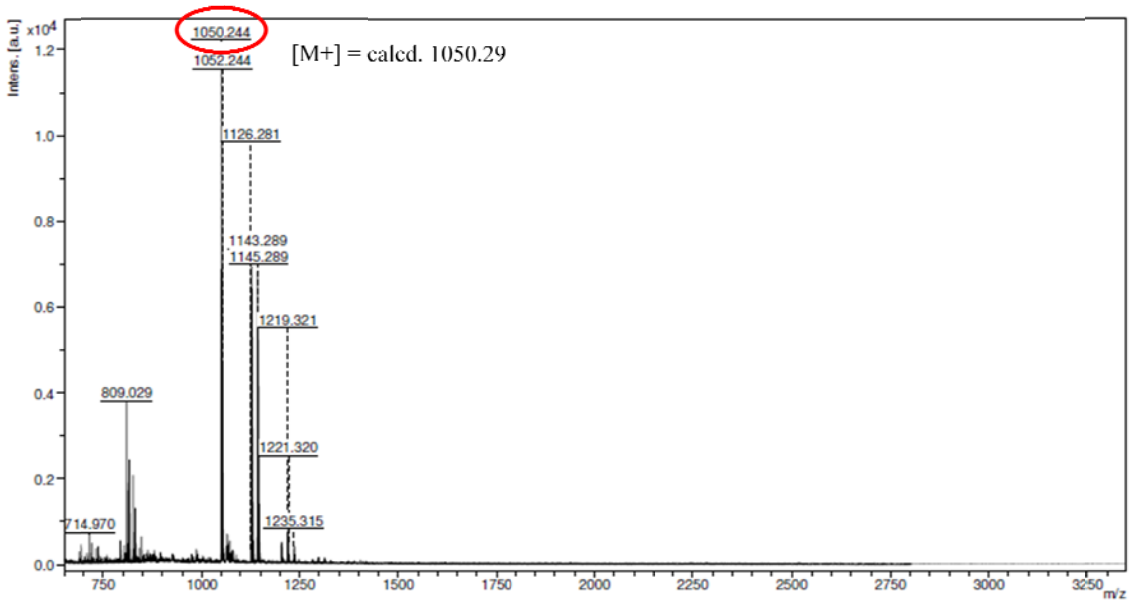

Figure S9. MALDI-TOF mass spectrum of NiOPP-MN (**3**).

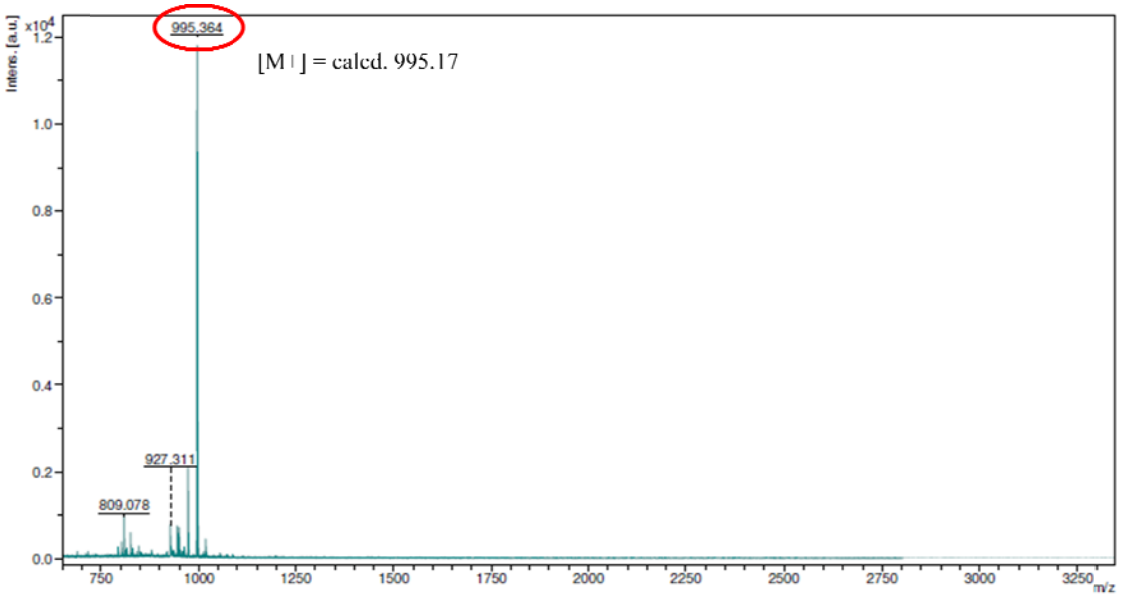

Figure S10. MALDI-TOF mass spectrum of H_2OPP-MN (**4**).

Table S1. Optical absorption spectral data of synthesized porphyrins in CH_2Cl_2 at 298 K.

Porphyrin	B band(s), nm	Q band(s), nm
H_2TPP-CHO	430(5.41)	525(4.16), 567(3.75), 604(3.64), 662(3.76)
NiTPP-CHO	427(5.32)	539(4.13), 580(4.01)
H_2OPP-CHO	450(4.40)	547(4.18), 594(4.01), 690(3.82)
NiOPP-CHO	444(5.28)	560(4.21), 605(3.97)
H_2TPP-MN	401(4.92), 453(5.24)	532(4.31), 580(3.97), 615(3.90), 675(3.98)
NiTPP-MN	385(4.82), 451(5.18)	550(4.07), 606(4.36)
H_2OPP-MN	469(5.20)	558(4.22), 608(3.99), 699(3.91)
NiOPP-MN	401(4.79), 465(5.20)	569(4.23), 627(4.32)

Values in parentheses refer to log ε (ε in Mol^{-1} cm^{-1})

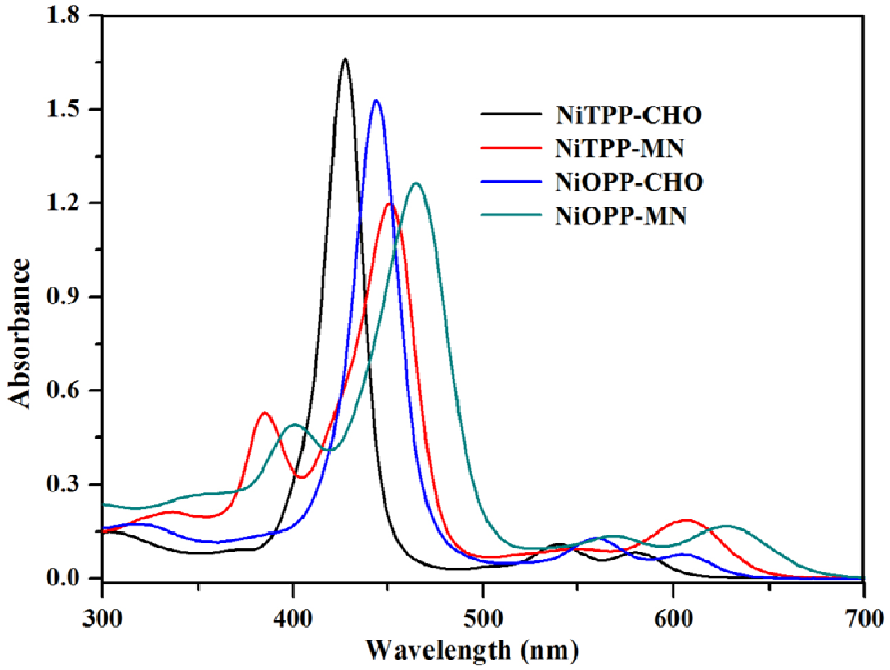

Figure S11. UV-Vis spectra of NiTPP-X (X = CHO, MN) derivatives in CH_2Cl_2 at 298 K.

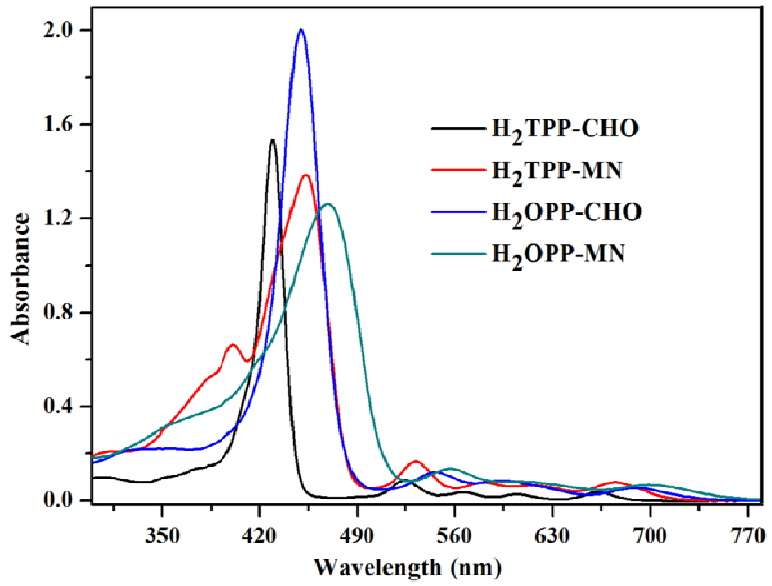

Figure S12. UV-Vis spectra of H_2TPP-X (X = CHO, MN) derivatives in CH_2Cl_2 at 298 K.

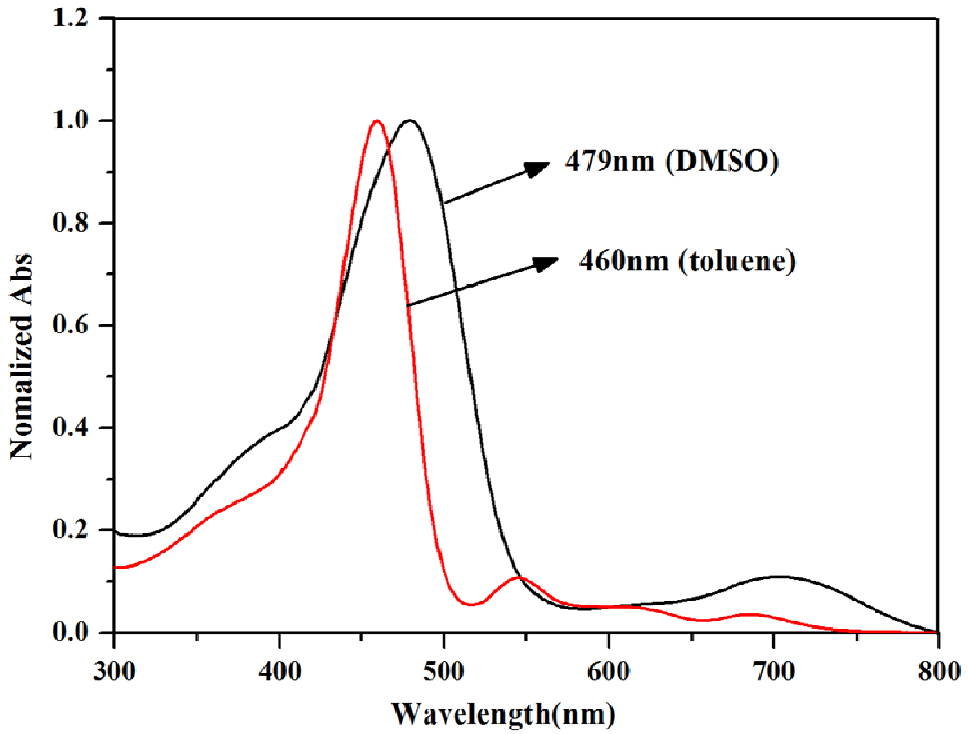

Figure S13. UV-Vis spectra of H_2OPP-MN (**4**) in toluene and DMSO (supports the nonplanar conformation as compared to H_2TPP-MN).

Table S2. Crystal data of NiTPP-MN (**1**)	
Empirical formula	$C_{48}H_{28}N_6Ni$
Formula Weight	747.45
Crystal system	triclinic
Space group	P –1
a (Å)	11.701(5)
b (Å)	13.019(5)
c (Å)	13.324(5)
α (°)	75.1
β (°)	69.33
γ (°)	85.16
Volume (Å^3)	1835.3(13)
Z	2
D_{cald} (mg/m^3)	1.353
Wavelength	0.71073
Temperature (K)	293 K
No. of total reflections	8893
No. of independent reflections	4287
R^a	0.0515
R_w^b	0.1669
CCDC	1401278

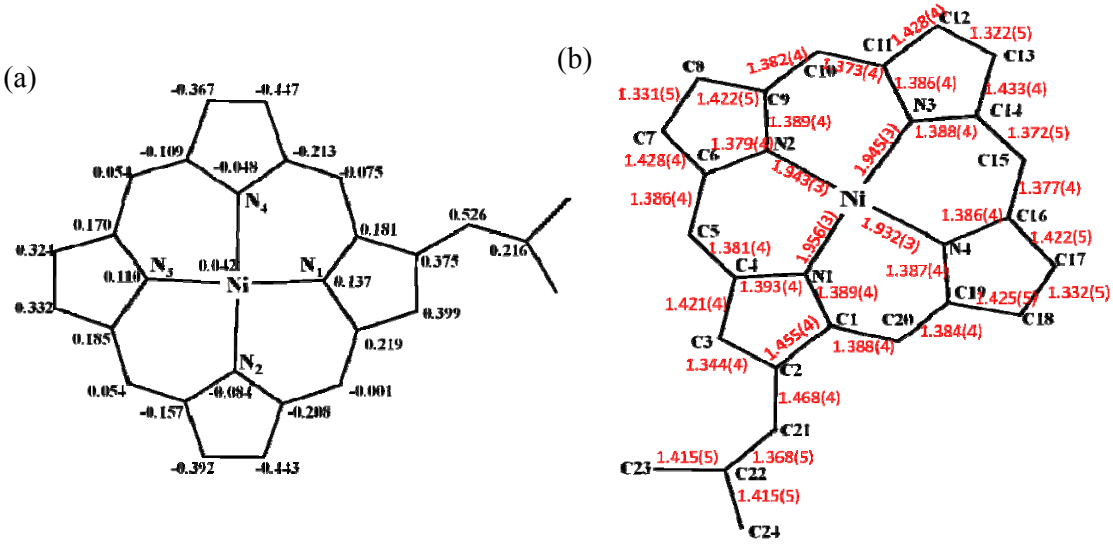

ΔC_β = 0.38 Å, Δ24 = 0.21 Å

Torsion angle (C3-C2-C21-C22) = 26.39°

Figure S14. (a) The displacement of porphyrin-core atoms in Å from the mean plane and (b) bond lengths of **1**.

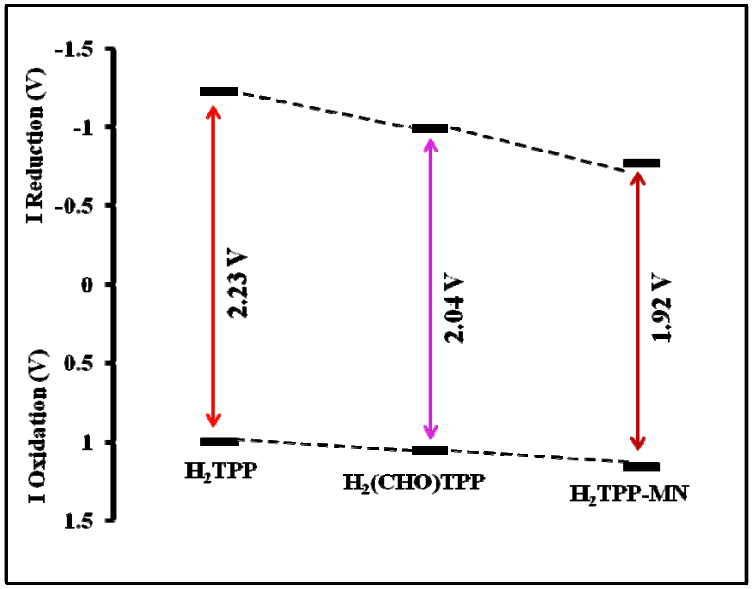

(a) Free-base TPP-system

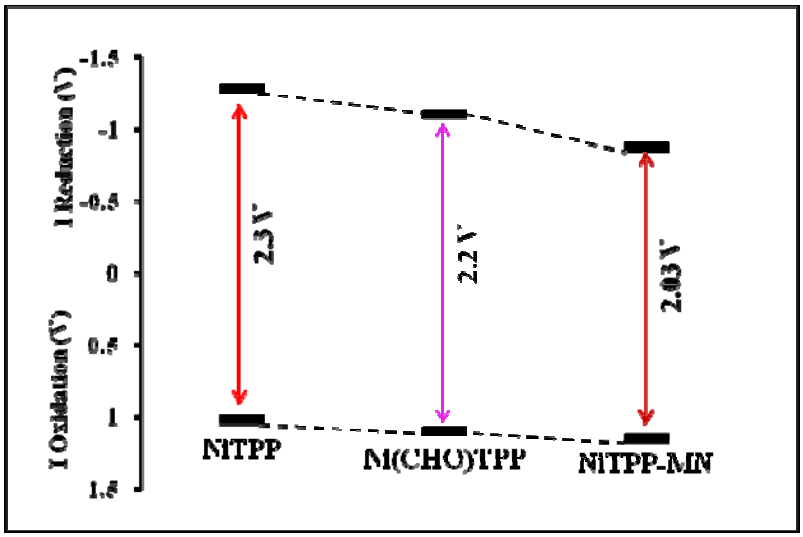

(b) Ni-metallated TPP-system

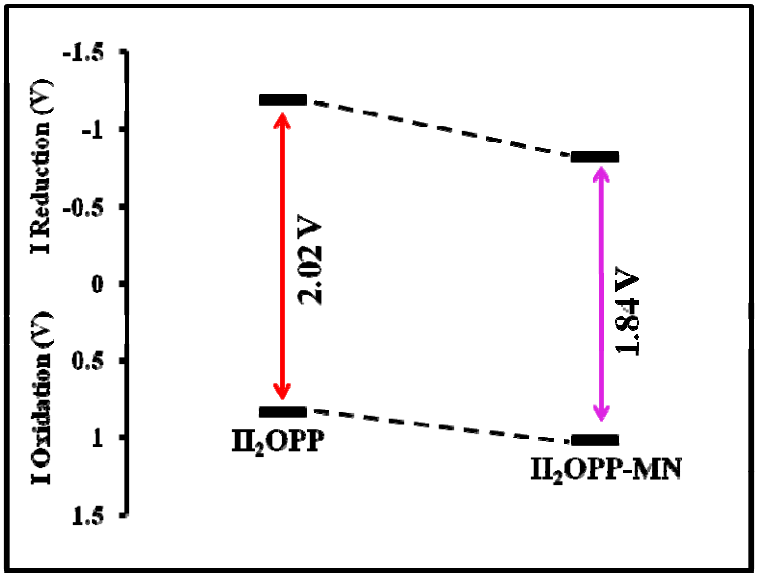

(c) Free-base OPP-system

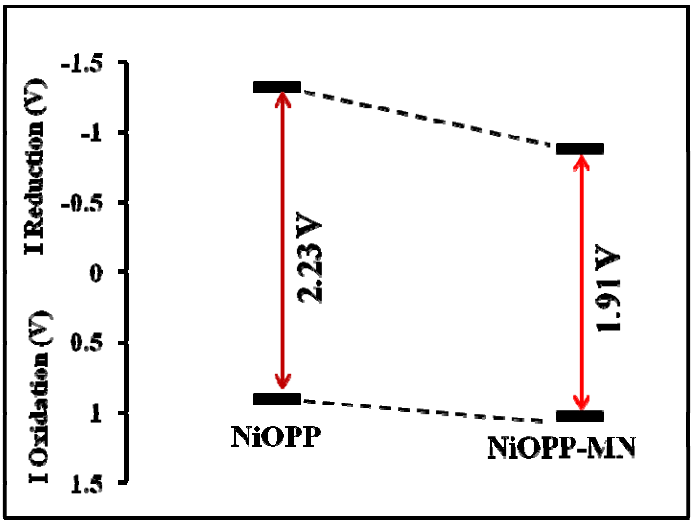

(d) Ni-metallated OPP-system

Figure S15. The HOMO-LUMO variation of various dicyanovinyl appended β-substituted porphyrins: (a) free-base TPP-system (b) Ni-metallated TPP-system (c) free-base OPP-system (d) Ni-metallated OPP-system.

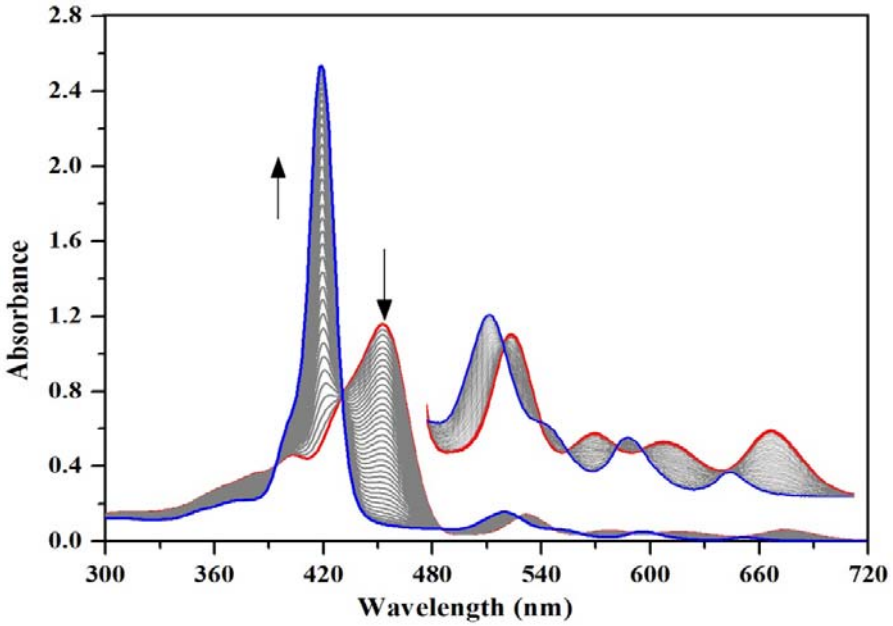

Figure S16. UV-Vis spectral response of **2** (8 μM) upon incremental addition of CN^- ions (1.3 equiv.) in toluene.

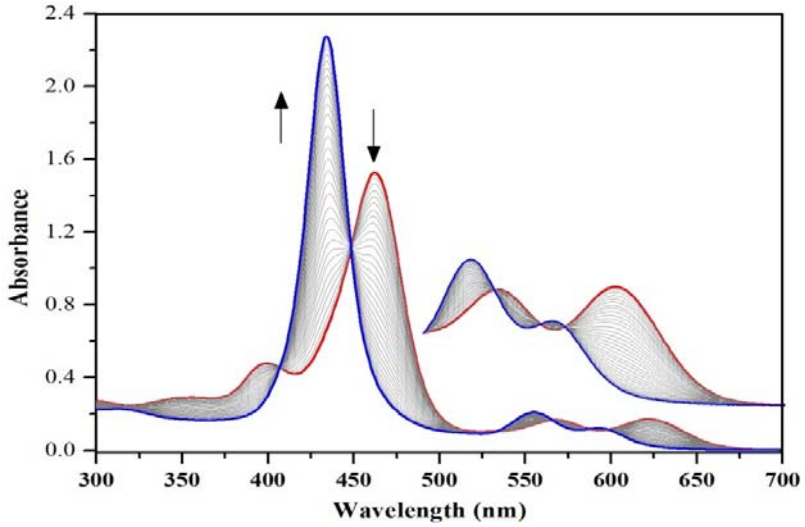

Figure S17. UV-Vis spectral response of **3** (8 μM) upon incremental addition of CN^- ions (2.5 equiv.) in toluene.

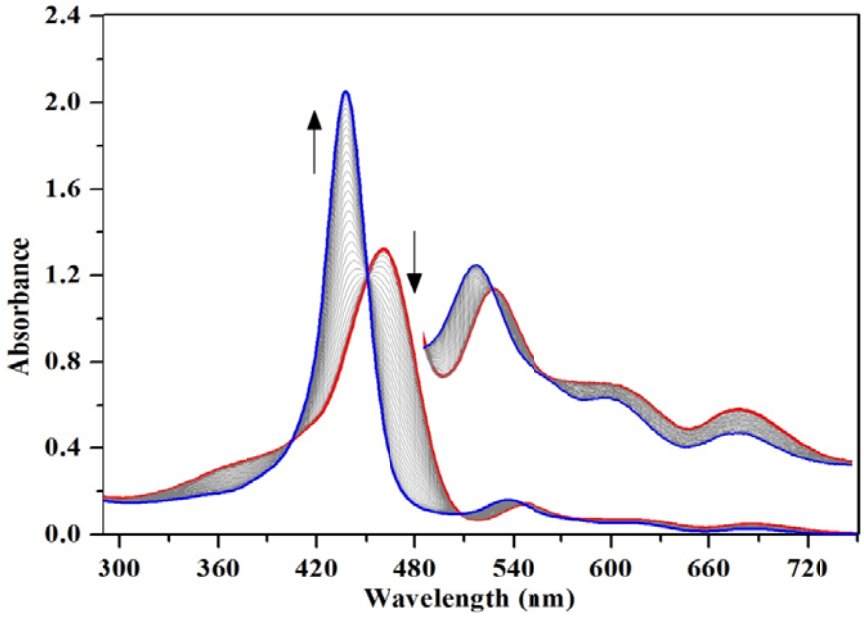

Figure S18. UV-Vis spectral response of **4** (8 μM) upon incremental addition of CN^- ions (2.3 equiv.) in toluene.

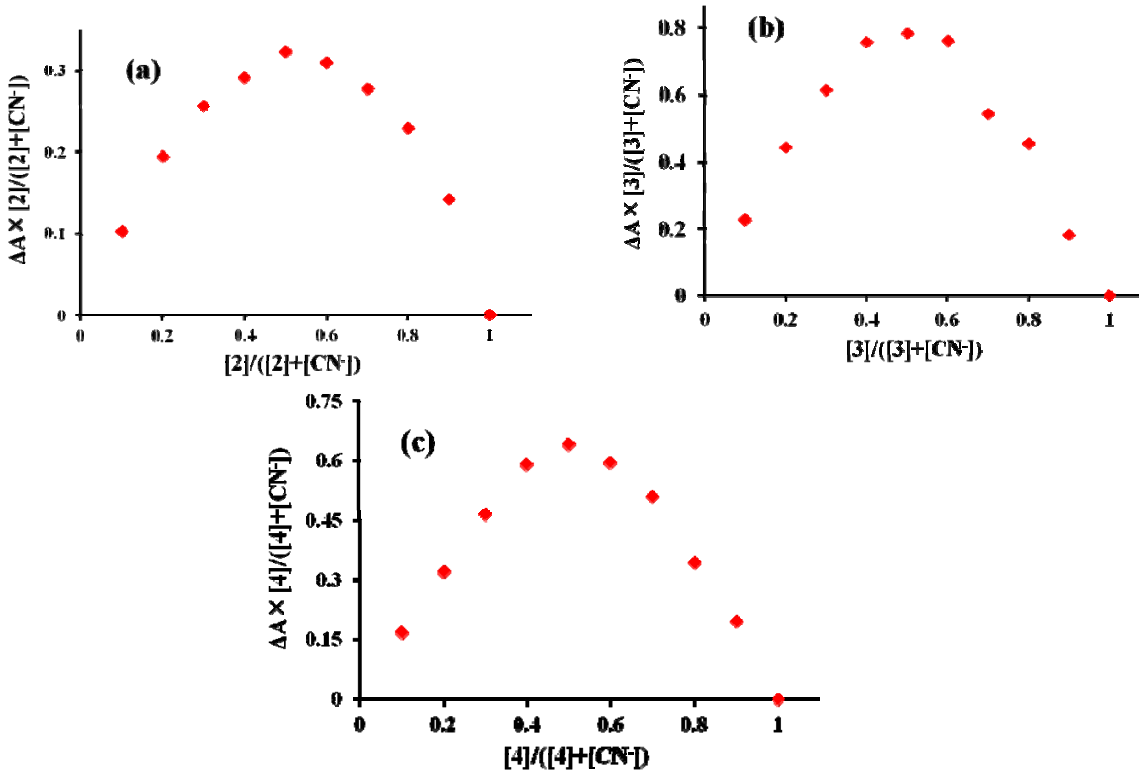

Figure S19. Job's plot for the porphyrin chemodosimeters.

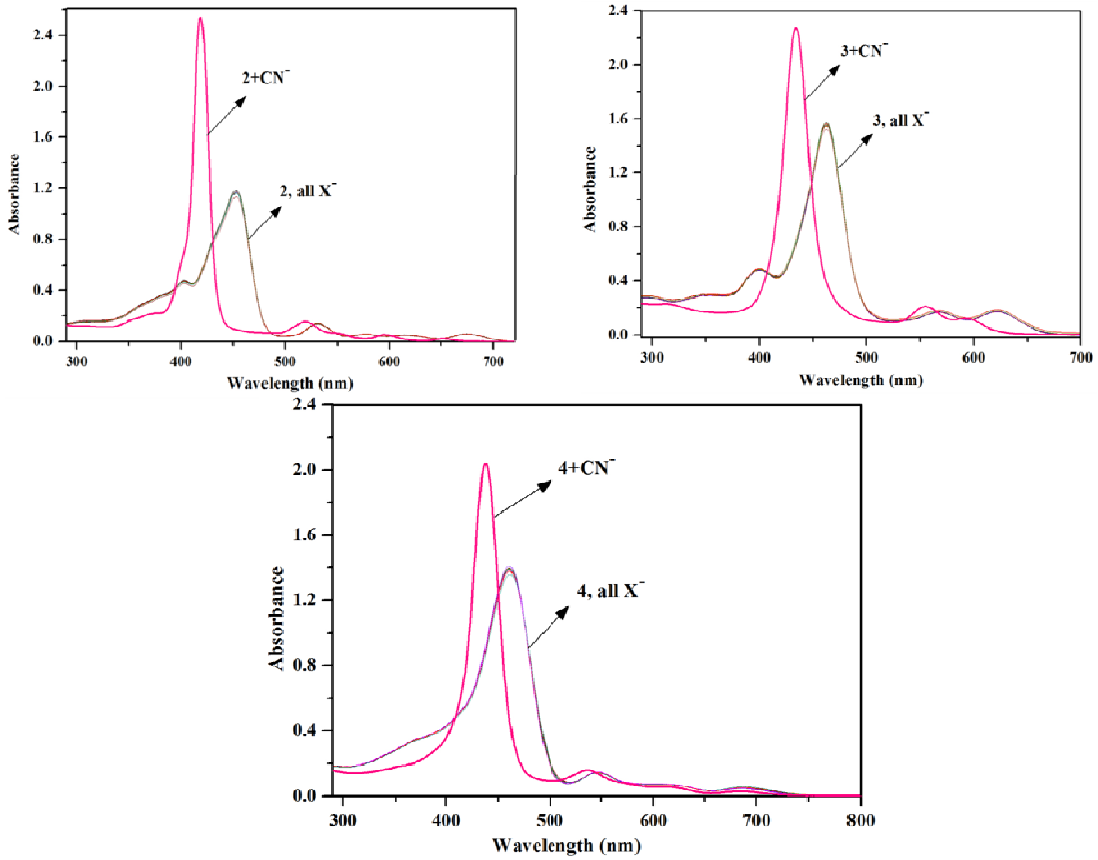

Figure S20. UV-Vis spectra of **2**, **3** and **4** in toluene upon addition of various anions.

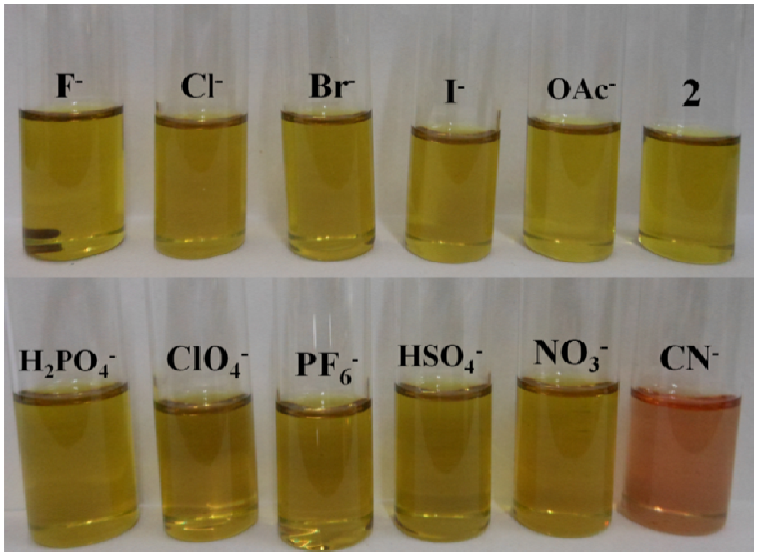

Figure S21. Visual-Colorimetric changes by addition of various anions to **2**.

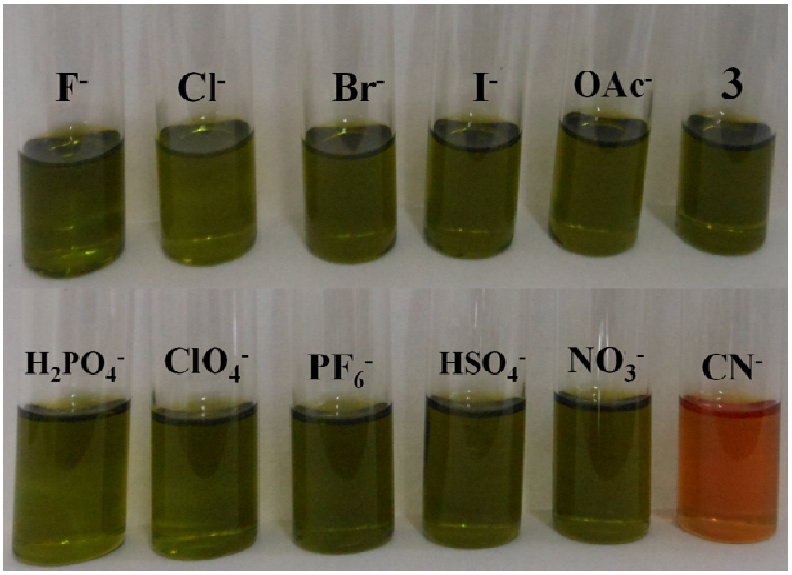

Figure S22. Visual-Colorimetric changes by addition of various anions to **3**.

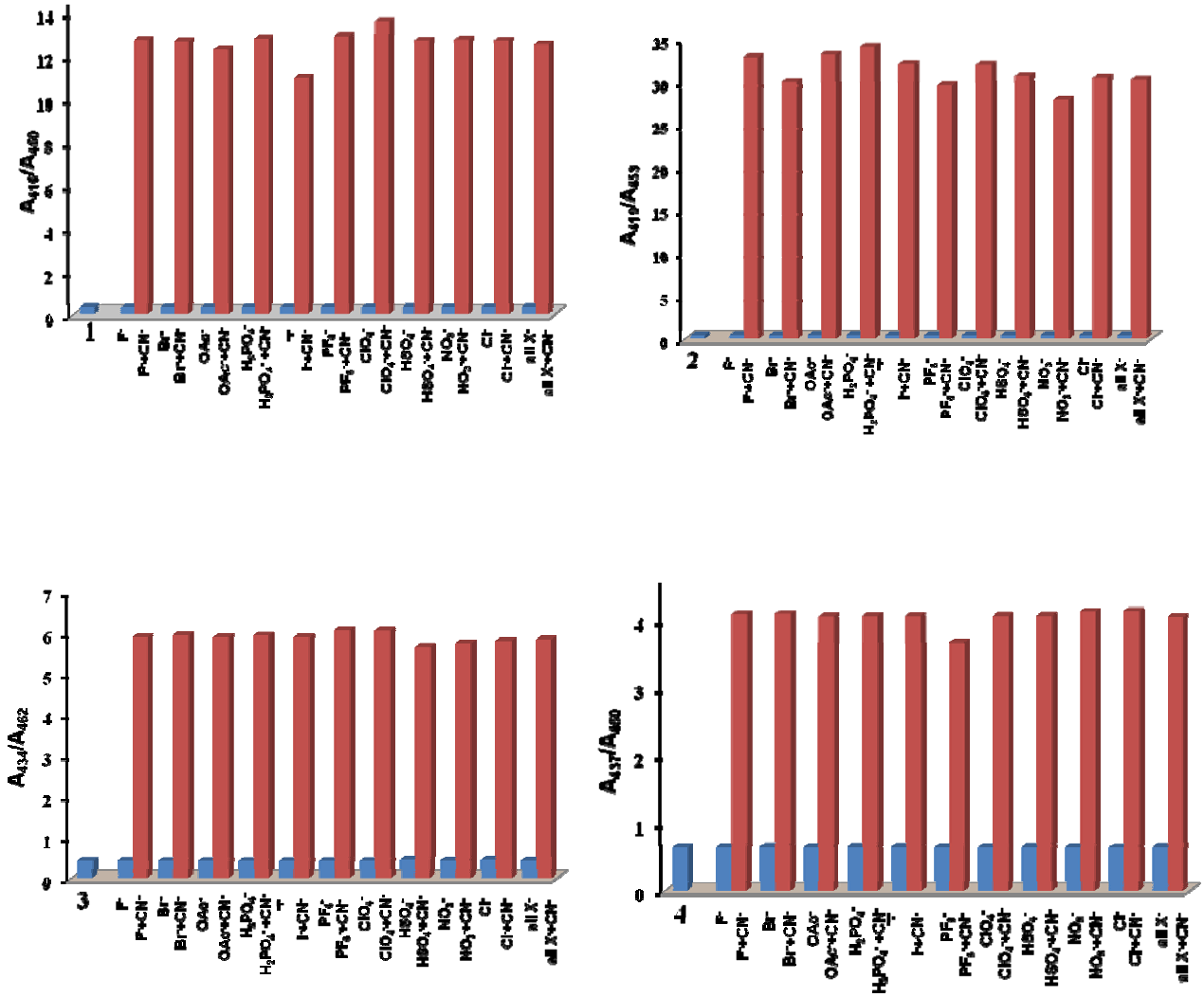

Figure S23. Ratiometric absorbance changes of **1**(A_{416}/A_{450}), **2**(A_{419}/A_{453}), **3**(A_{434}/A_{462}) and **4**(A_{437}/A_{460}) upon addition of CN^- ions and 10 equiv. of other anions. Blue bars indicate the blank and various anions, and red bars indicate the addition of CN^- ions to the interfering anions.

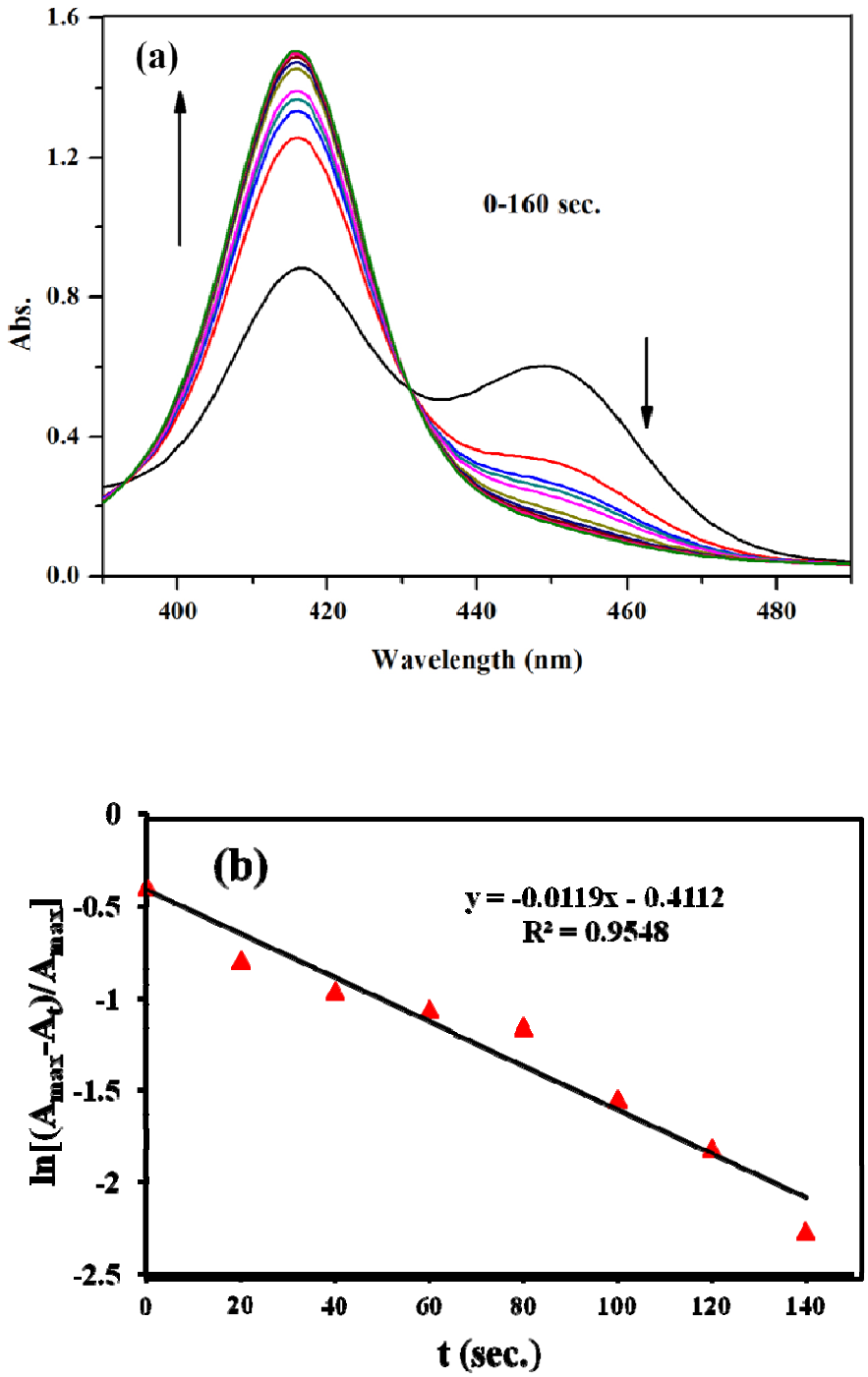

Figure S24. (a) Changes in absorption spectra of **1** incubated with CN^- ions for 0–160 seconds. (b) Pseudo-first-order kinetic plot.

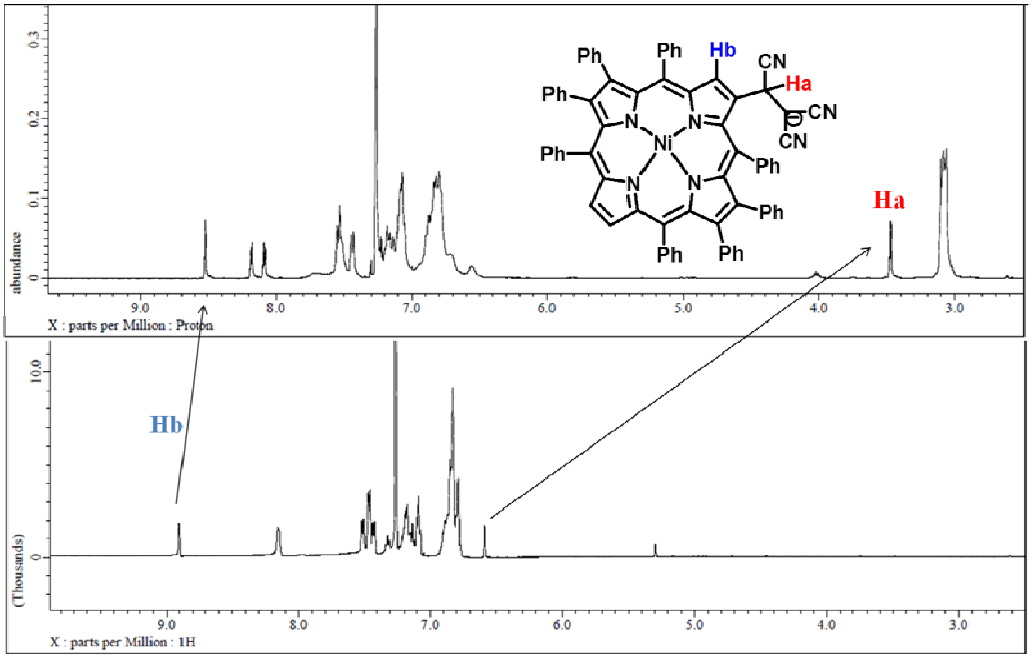

Figure S25. ^{1}H NMR spectra of the adduct **[3-CN]**$^{-}$ after addition of CN^{-} ions (1 equiv.) to NiOPP-MN (5×10^{-3} M).

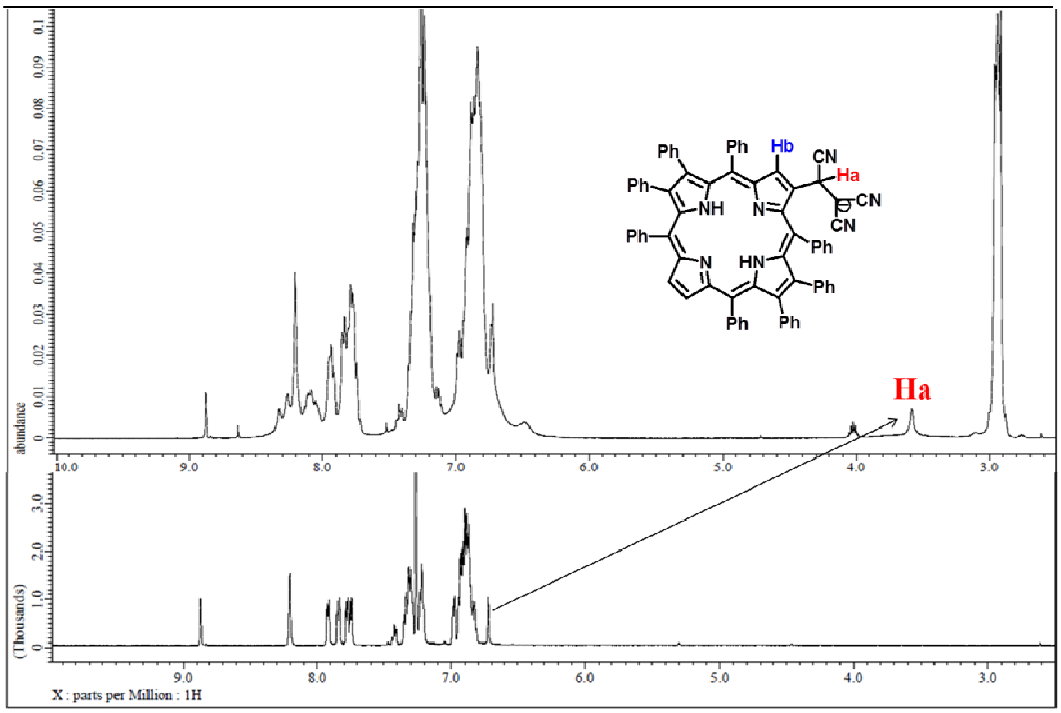

Figure S26. ^{1}H NMR spectra of the adduct **[2-CN]**$^{-}$ after addition of CN^{-} ions (1 equiv.) to H_2TPP-MN (5×10^{-3} M).

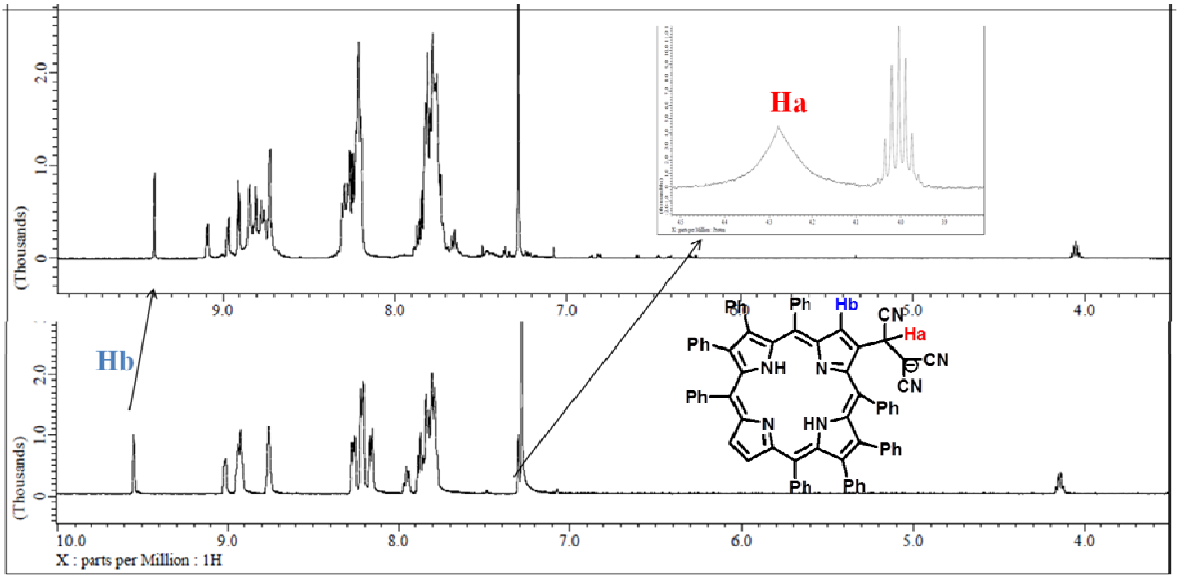

Figure S27. ^{1}H NMR spectra of the adduct **[4-CN]**$^{-}$ after addition of CN^{-} ions (1 equiv.) to H_2OPP-MN (5×10^{-3} M).

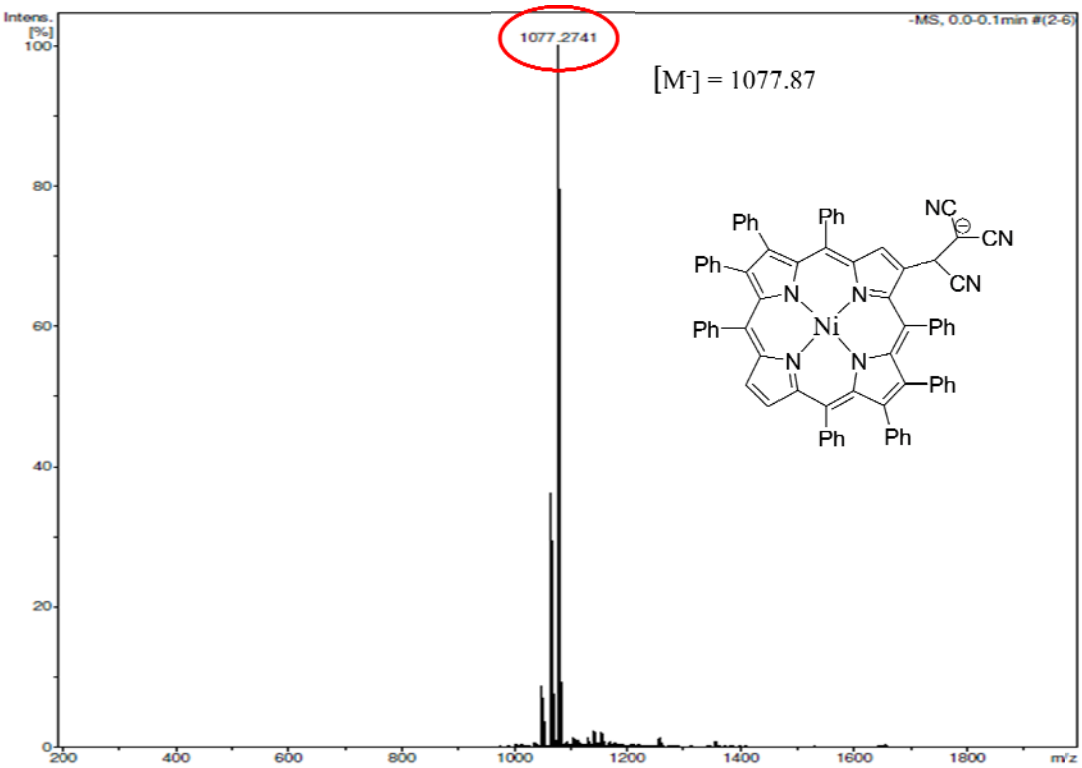

Figure S28. ESI-MS spectrum of the adduct **[3-CN]**$^{-}$ after addition of CN^{-} ions (1 equiv.) to NiOPP-MN (**3**).

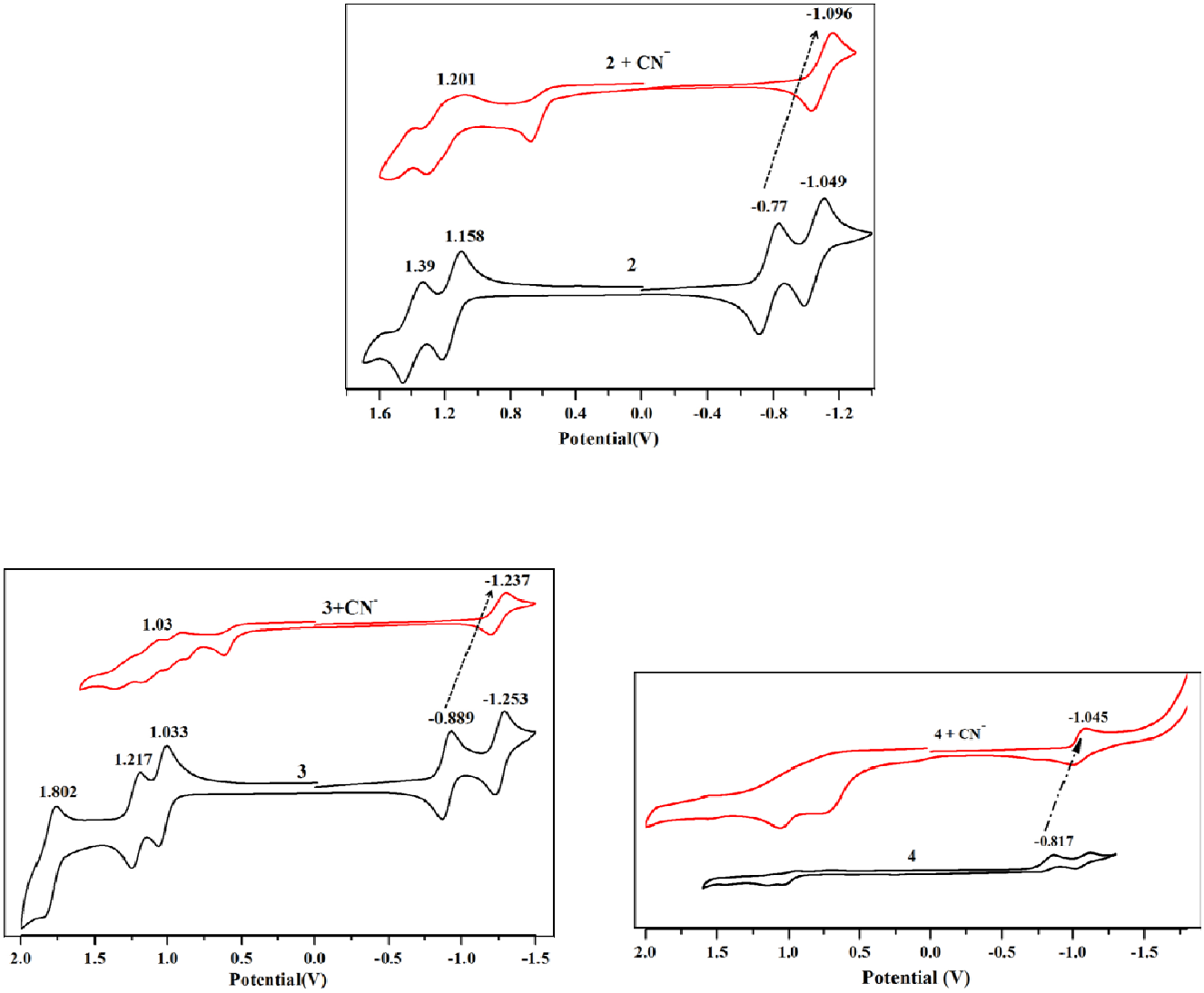

Figure S29. Cyclic voltametric studies of **2-4** in absence and presence of [CN^-] in CH_2Cl_2 containing 0.1 M $TBAPF_6$ at 298 K.

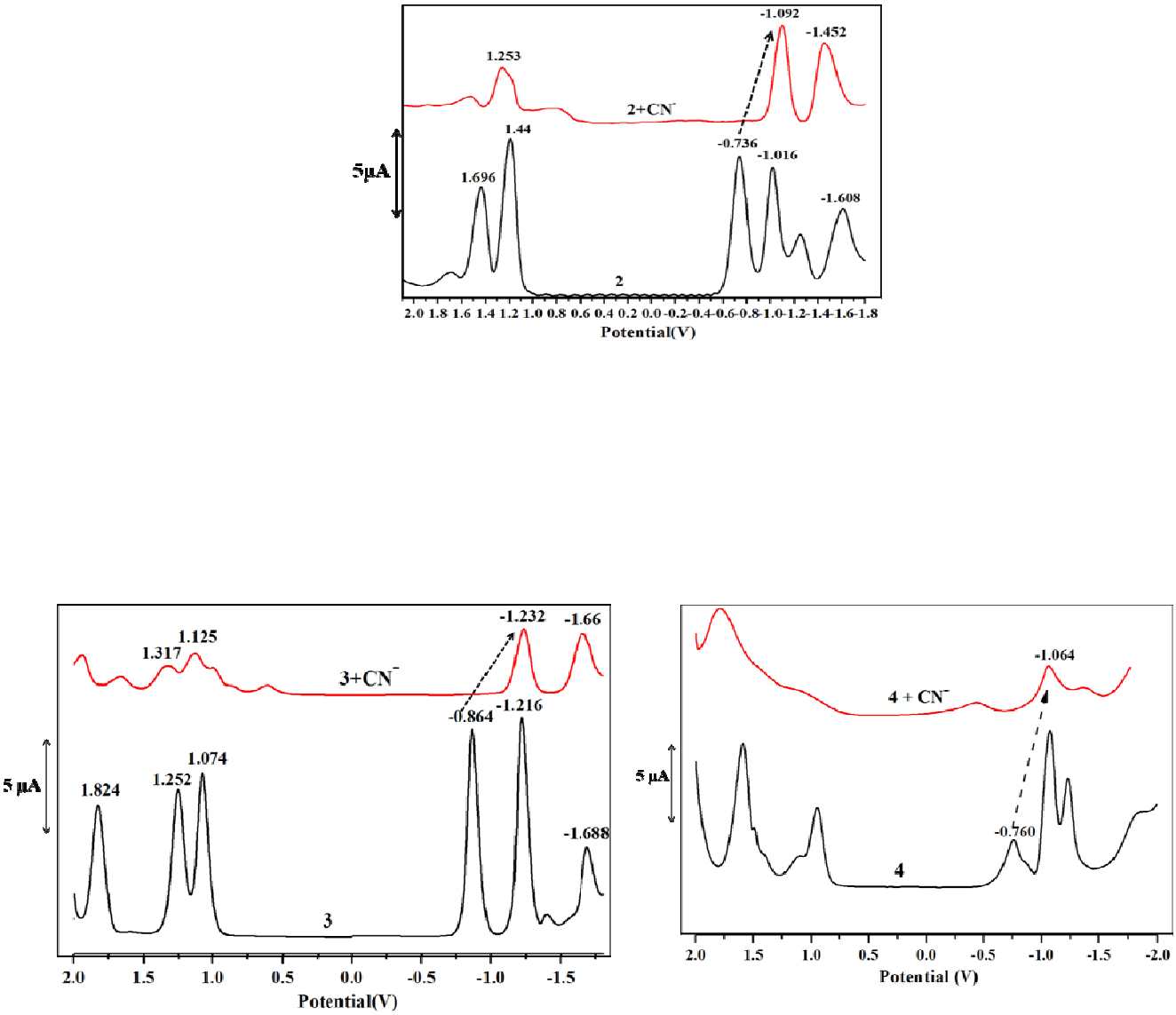

Figure S30. DPV traces of **2-4** in absence and presence of [CN^-] in CH_2Cl_2 containing 0.1 M $TBAPF_6$ at 298 K.

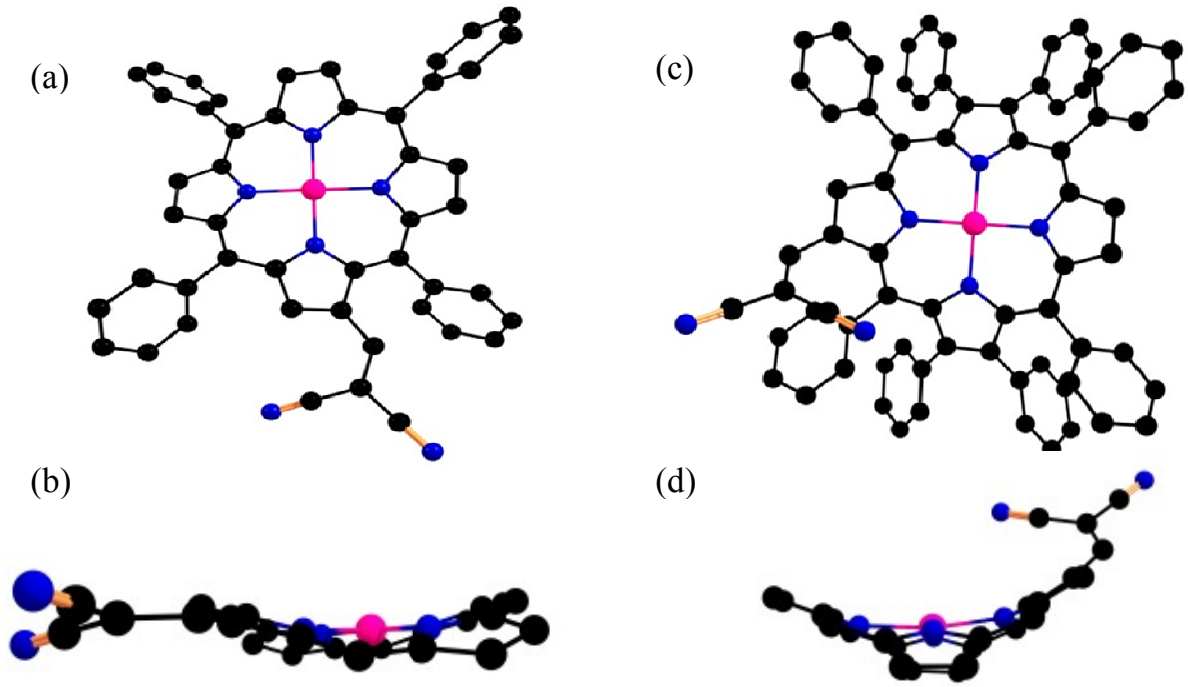

Figure S31. Optimized-geometries showing top as well as side views of NiTPP-MN (a and b) and NiOPP-MN (c and d), respectively.

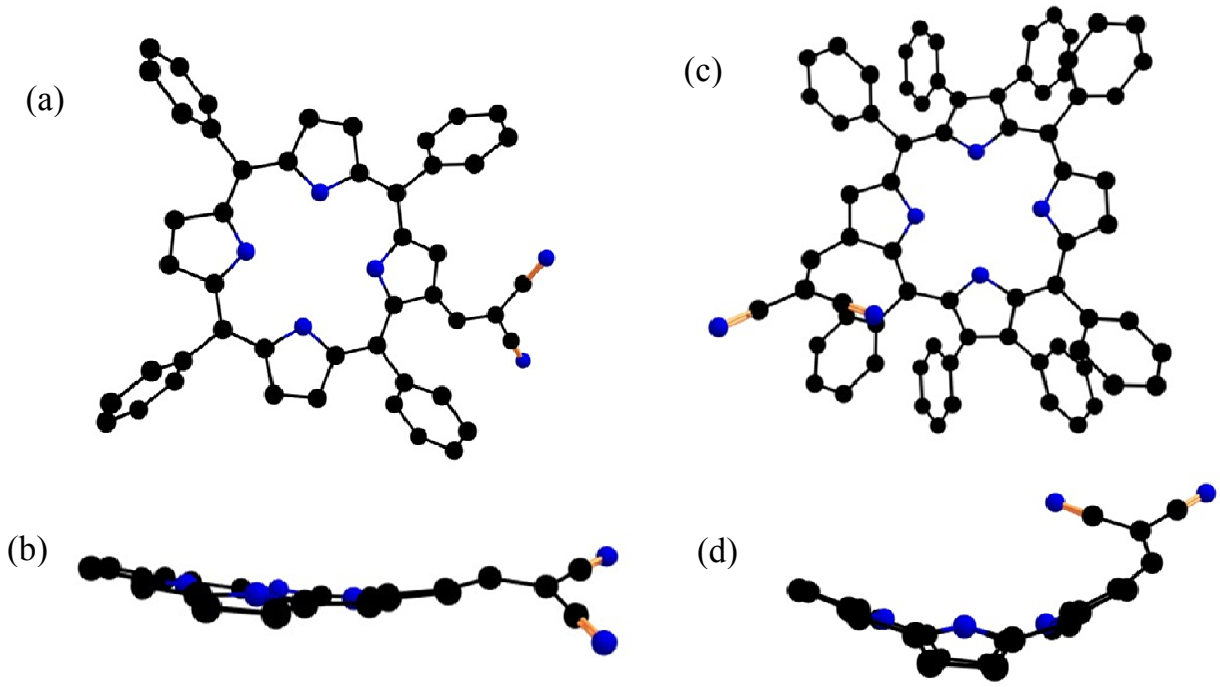

Figure S32. Optimized-geometries showing top as well as side views of H_2TPP-MN (a and b) and H_2OPP-MN (c and d), respectively.

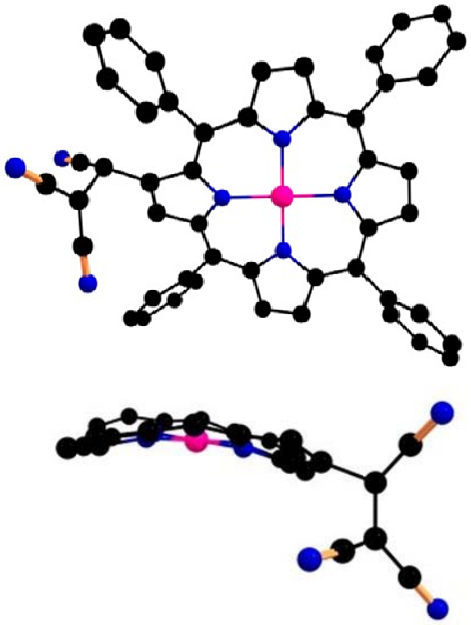

NiTPP-MN(**1**)-CN$^-$

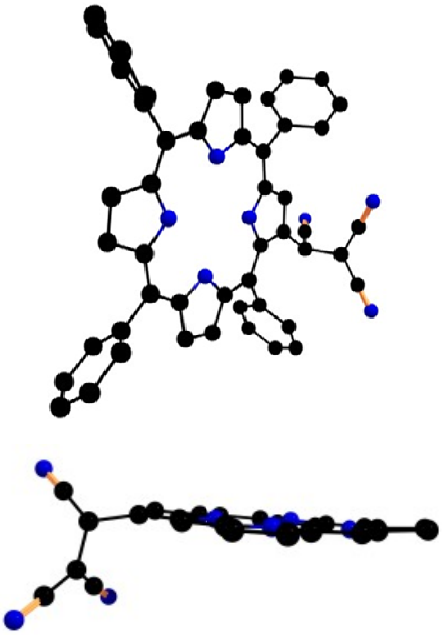

H_2TPP-MN(**2**)-CN$^-$

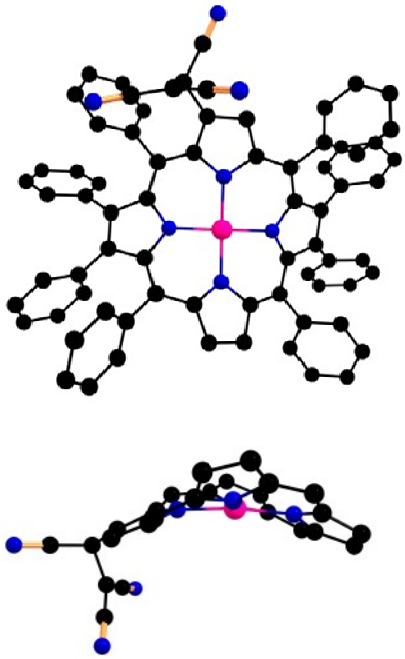

NiOPP-MN(**3**)-CN$^-$

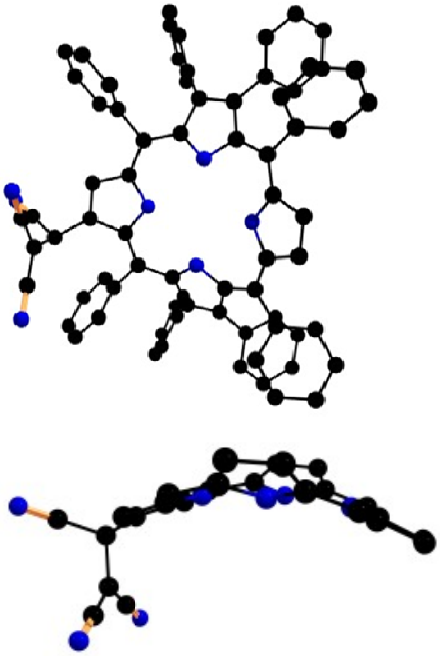

H_2OPP-MN(**4**)-CN$^-$

Figure S33. Optimized-geometries for **1-CN$^-$, 2-CN$^-$, 3-CN$^-$** and **4-CN$^-$**.

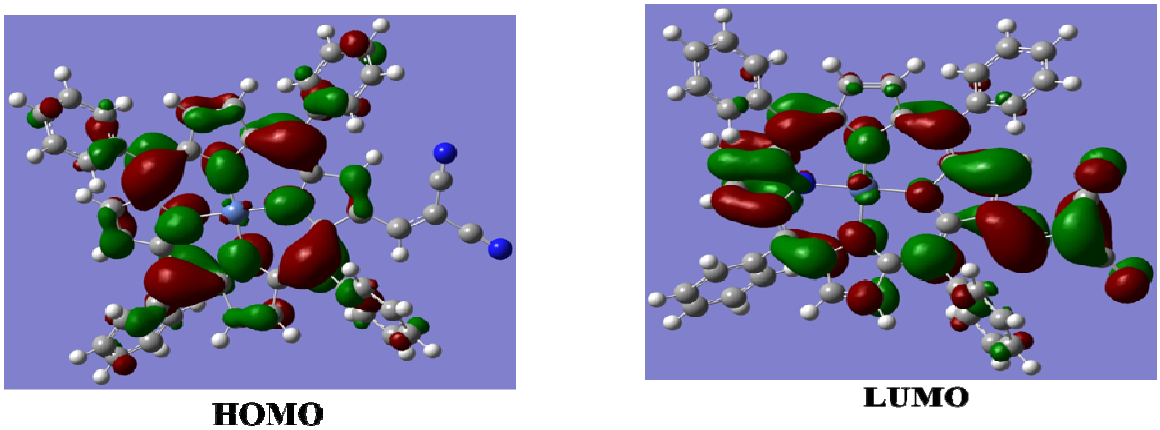

Figure S34. Pictorial representation of frontier orbitals of NiTPP-MN (**1**).

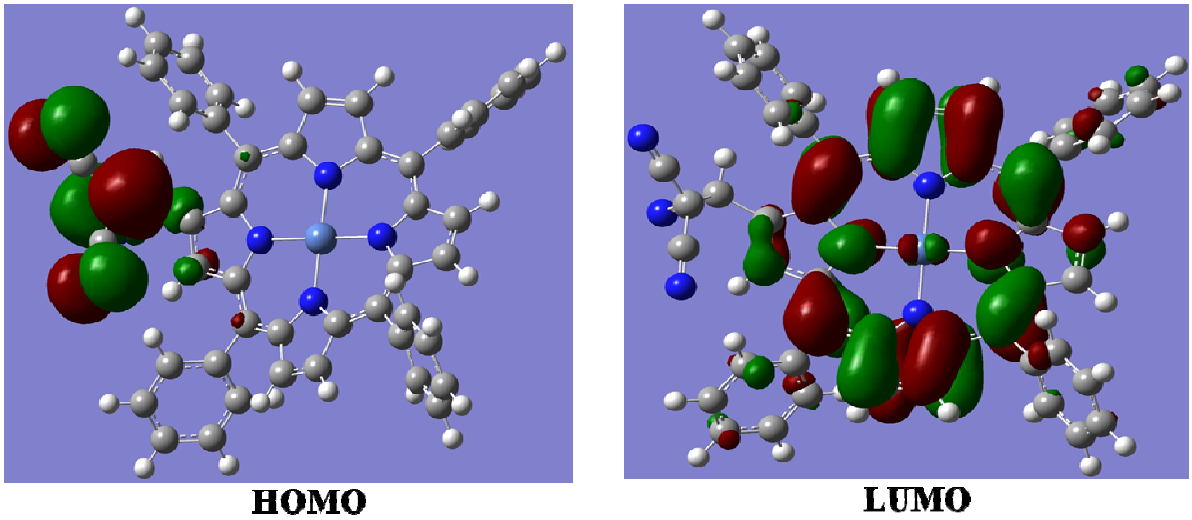

Figure S35. Pictorial representation of frontier orbitals of anionic species formed after the addition of CN^- to NiTPP-MN (**1**).

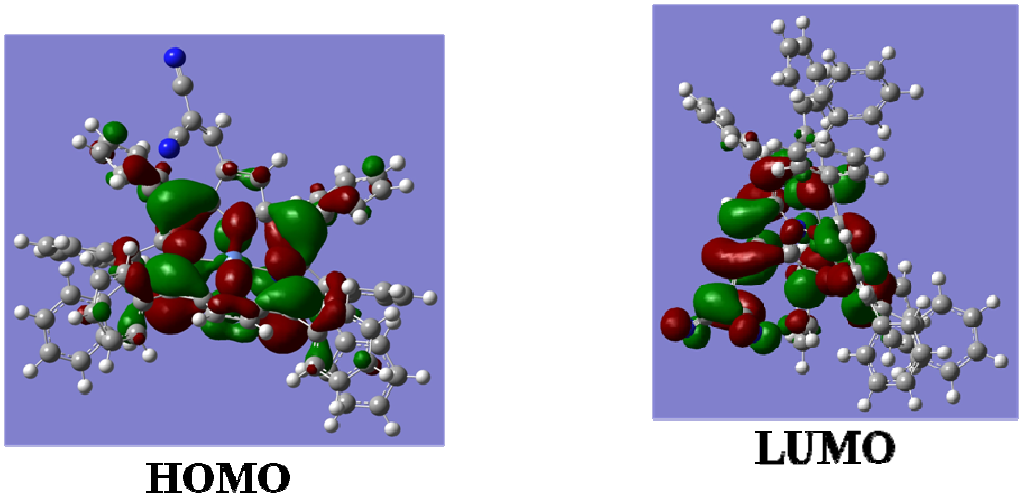

Figure S36. Pictorial representation of frontier orbitals of NiOPP-MN (**3**).

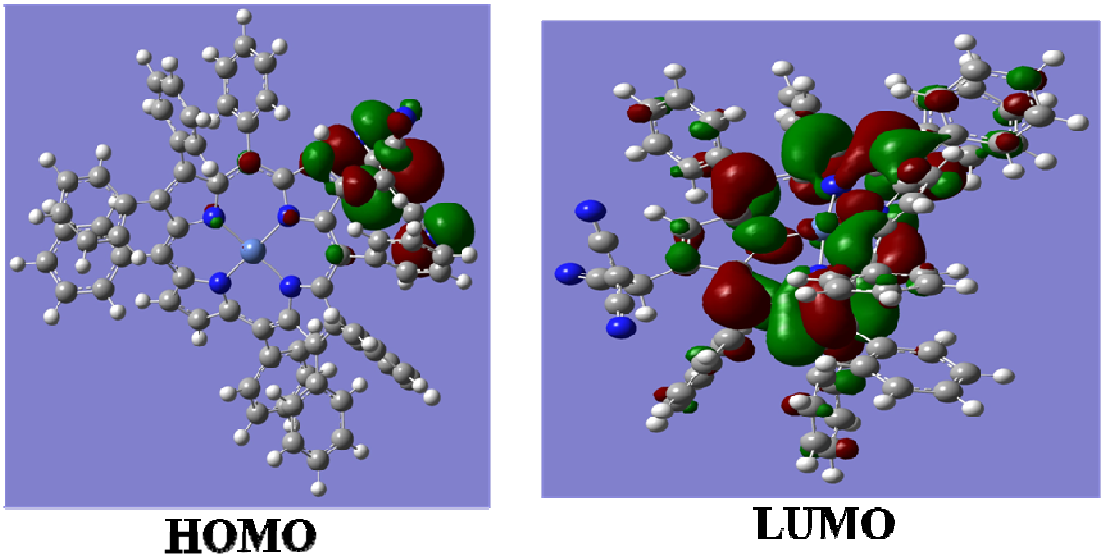

Figure S37. Pictorial representation of frontier orbitals of anionic species formed after the addition of CN^- to NiOPP-MN (**3**).

Table S3. Deviation of β-pyrrole carbons (Å) and 24 core atoms from porphyrin mean plane (Å) and torsion angle (º) between β-pyrrole ring of porphyrin and dicyanovinyl substituent.

Porphyrin	Deviation(Å)	Torsion angle (º)
NiTPP-MN	$\Delta C_\beta = 0.380$ $\Delta 24 = 0.308$	23.5
H_2TPP-MN	$\Delta C_\beta = 0.292$ $\Delta 24 = 0.135$	27.2
NiOPP-MN	$\Delta C_\beta = 1.064$ $\Delta 24 = 0.54$	38.0
H_2OPP-MN	$\Delta C_\beta = 0.924$ $\Delta 24 = 0.446$	43.7
NiTPP-MN + CN^-	$\Delta C_\beta = 0.224$ $\Delta 24 = 0.277$	77.5
H_2TPP-MN + CN^-	$\Delta C_\beta = 0.101$ $\Delta 24 = 0.052$	79.1
NiOPP-MN + CN^-	$\Delta C_\beta = 0.938$ $\Delta 24 = 0.54$	81.1
H_2OPP-MN + CN^-	$\Delta C_\beta = 0.892$ $\Delta 24 = 0.427$	91.7

ΔC_β refers mean plane deviation of β-carbon atoms, $\Delta 24$ refers mean plane deviation of 24 core atoms.

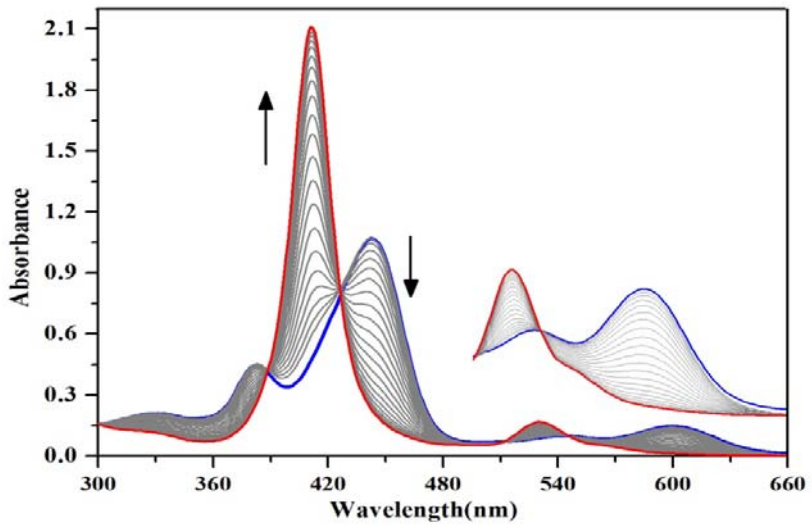

Figure S38. UV-Vis spectral response of **1** (8 μM) upon incremental addition of CN^- ions (0-3.15 × 10^{-4} M) in 10% H_2O:MeCN.

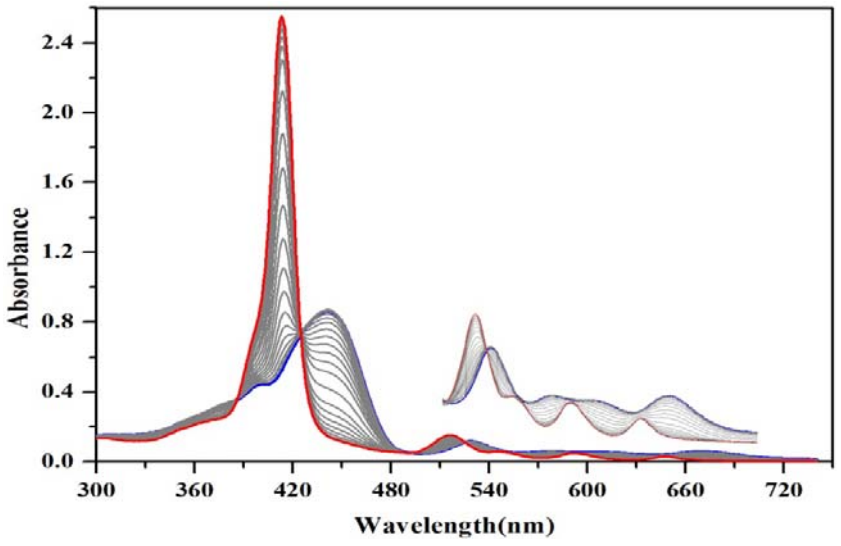

Figure S39. UV-Vis spectral response of **2** (8 μM) upon incremental addition of CN^- ions (0-3.45 × 10^{-4} M) in 10% H_2O:MeCN.

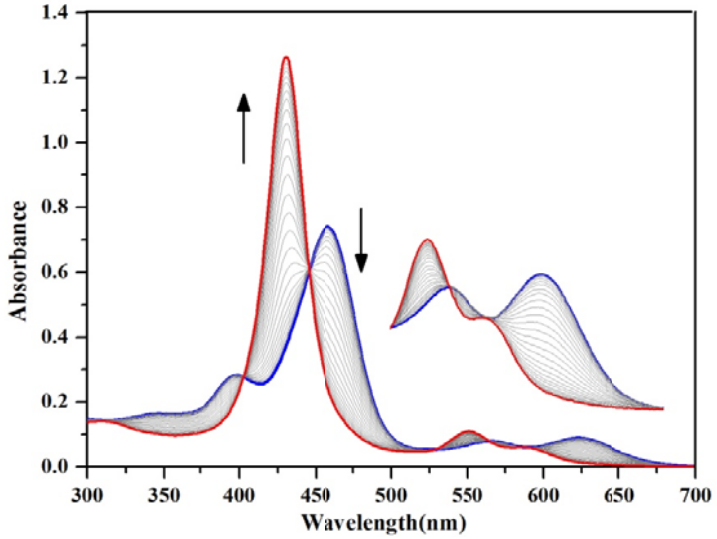

Figure S40. UV-Vis spectral response of **3** (8 μM) upon incremental addition of CN^- ions (0-4.33 × 10^{-4} M) in 10% H_2O:MeCN.

Table S4. Detection limits (LOD) in toluene and 10% H_2O:CH_3CN at 298 K.

Porphyrin	LOD (toluene) (in ppm)	LOD (H_2O:CH_3CN) (in ppm)
NiTPP-MN(**1**)	0.082	1.64
H_2TPP-MN(**2**)	0.023	1.84
NiOPP-MN(**3**)	0.073	1.76
H_2OPP-MN(**4**)	0.058	-

(a) (b)

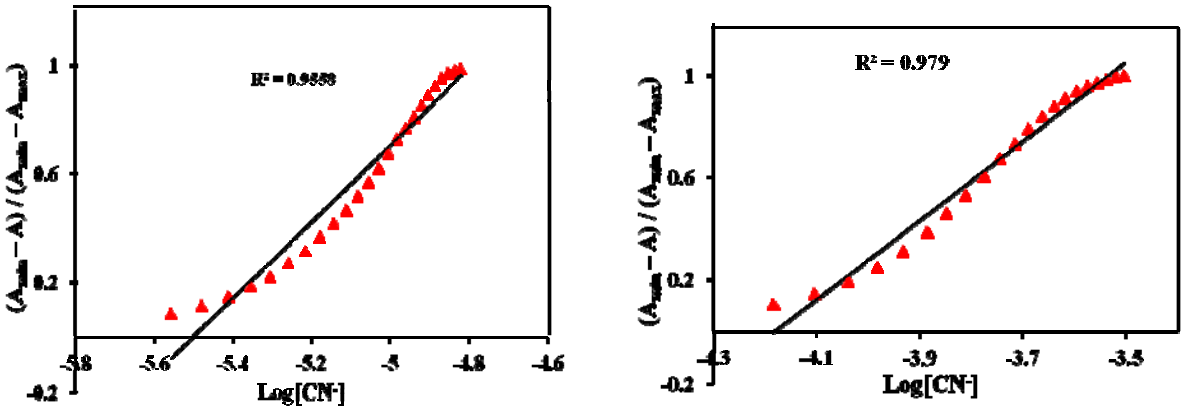

Figure S41. Absorbance of NiTPP-MN (**1**), normalized between the minimum absorbance found at zero equiv. of CN^- and the maximum absorbance (a) in toluene and (b) in 10% H_2O:CH_3CN.